Nonlinear Constitutive Modelling of in-Filled Concrete in Square CFST Columns

S. K. Katariya¹; Amit Rautela²; Pankaj Prasad³

¹Associate Professor, ²M.Tech. Student, ³Assistant Professor

¹Department of Civil Engineering, C.O.T., G.B.P.U.A. & T. Pantnagar, India

Publication Date: 2025/11/27

Abstract: This study presents a comprehensive nonlinear constitutive model for the in-filled concrete of square Concrete-Filled Steel Tube (CFST) columns, accounting for the confinement effects provided by the steel tube. Due to the non-uniform confinement in square sections particularly reduced effectiveness in flat regions compared to corners—the behaviour of the core concrete differs significantly from that observed in circular CFST columns. To capture this response, an effective lateral confining pressure model is formulated, incorporating tube thickness, yield strength, and confinement efficiency. The confined concrete strength and strain capacity are derived using an enhanced Mander-type relationship, and a continuous nonlinear stress—strain equation is proposed to represent both the ascending and descending branches of the concrete response. The model enables the generation of complete constitutive curves suitable finding the axial capacity of square CFST columns. Validation against experimental data from the literature demonstrates that the proposed formulation predicts peak stress and overall axial behaviour of square CFST columns. The model provides a reliable analytical tool for structural designers and researchers for simulating the nonlinear compression behaviour of concrete infill in square CFST systems.

Keywords: CFST Column, Axial Compression, Confinement, Nonlinear Behaviour.

How to Cite: S. K. Katariya; Amit Rautela; Pankaj Prasad (2025) Nonlinear Constitutive Modelling of in-Filled Concrete in Square CFST Columns. *International Journal of Innovative Science and Research Technology*, 10(11), 1592-1601. https://doi.org/10.38124/ijisrt/25nov1123

I. INTRODUCTION

Concrete-Filled Steel Tube (CFST) columns have gained significant prominence in modern structural engineering due to their superior axial capacity, enhanced ductility, and efficient composite action between steel and concrete. While extensive research has been conducted on circular CFST columns, square CFST columns continue to receive increasing attention because of their architectural compatibility and suitability for modular construction systems. However, unlike circular sections, square CFST columns exhibit highly non-uniform confinement, with strong confinement concentrated in the corner regions and weaker restraint along the flat faces of the steel tube. This non-uniformity results in a complex stress distribution in the in-filled concrete, making its behaviour difficult to capture using conventional confined concrete models.

Accurate representation of the concrete infill is crucial for predicting the axial response, stiffness degradation, ductility, and overall load-carrying mechanism of square CFST members. Many existing models either oversimplify the confinement mechanism or are primarily calibrated for circular sections, leading to limited applicability for square geometries. The nonlinear behaviour of the confined concrete

characterised by enhanced compressive strength, increased strain capacity, and a modified post-peak softening response—requires a constitutive model that accounts explicitly for the geometric and mechanical interactions unique to square steel tubes.

In this context, the present study develops a nonlinear constitutive model specifically tailored for in-filled concrete in square CFST columns. The model incorporates an effective lateral confinement formulation based on tube thickness, yield strength, and confinement efficiency, recognising the reduced effectiveness along flat faces. Using an improved Mander-type framework, the proposed model predicts the confined compressive strength, peak strain, and the full nonlinear stress–strain relationship necessary for finite element simulations.

The outcomes of this work contribute to improved analytical tools for CFST design, allowing researchers and engineers to better simulate axial performance, optimise material usage, and enhance the reliability of square CFST column applications in contemporary structural systems. The mechanical behaviour of confined concrete has been extensively studied, with foundational contributions by Mander et al. [1]. Finite element analyses by Schneider [2]

ISSN No:-2456-2165

and Ge and Usami [3] have provided deeper insight into the axial behaviour of concrete-filled steel tube members. Building on these developments, Han [4] introduced a unified confinement theory in which a confinement factor (ξ) quantifies the composite interaction between the steel tube and the concrete infill. Several studies have examined the behaviour of square CFST columns incorporating highstrength concrete (HSC) [5,6]. These investigations reported that column ductility decreases markedly with increasing axial load ratio. However, research on square spiral-confined concrete-filled steel tube (SCCFST) columns remains limited. Ding et al. [7] conducted axial compression tests on six SCCFST specimens (concrete strength $f_c' = 60$ MPa), and their results indicated that the inclusion of spiral reinforcement enhances both axial capacity and ductility, with the improvement becoming more pronounced as the spiral volumetric ratio increases. Teng et al. [8] performed axial compression tests on SCCFST columns with concrete strengths ranging from 34 to 80 MPa. Their findings showed that high-strength spiral reinforcement improves the compressive strength, although the degree of enhancement diminishes at higher concrete strengths. Chen et al. [9] tested twenty SCCFST columns ($f_c' = 24-40$ MPa) under axial loading and reported that increasing the steel content of spiral reinforcement has a more significant influence on loadcarrying capacity and ductility than increasing the steel content of the square tube itself, when the total steel amount is kept constant. Tan et al. [10] carried out eccentric compression tests on seventeen SCCFST specimens ($f_c' = 30$ MPa), and observed that the spiral reinforcement yielded when the column reached its peak axial load.

II. MATERIALS AND METHOD

Using the approaches, a mechanics-based model was proposed for in-filled concrete to predict the behaviour of concrete-filled square FCST columns under axial compression. The experimental data for square concrete-filled steel tubes were taken from various research papers.

The axial load -strain curves from research papers were selected, cropped and digitized. The stress-strain behaviour for steel for adopted as provided by Han et al. [11]. The load taken by in-filled concrete is calculated by assuming the load taken by section of steel tubes at yield point of steel. The stress in concrete was obtained using load taken by concrete and corresponding sectional area of concrete. The stresses in concrete were obtained for selected values of strain in concrete.

There are number of factors on which the confinement effect depends like, size of section, grade of steel and in-filled concrete and side length of section to thick of steel tubes ratio.

A wide range of specimens was considered in this study to examine the behaviour of square CFST columns. The newly developed equation, formulated through regression analysis and refined with the corrections discussed in the previous chapter, is employed to predict the load—axial strain response of square CFST columns. The predicted curves generated using this equation are then compared with the corresponding experimental load—axial strain curves reported in previous research studies. In addition, the predicted peak load values are evaluated against the experimental peak loads to assess the accuracy and reliability of the proposed model. The equation for the stress in concrete as given by Han et al. was modified in the following manner.

➤ Approach Towards the Equation

To develop the required equation, the first step was to identify the key parameters that govern the load—axial strain response of square CFST columns. After analyzing all influencing variables, it was observed that three parameters predominantly control the shape and behavior of the curve. Each of these parameters was then multiplied by a suitable modification factor so that the numerical curve matched the corresponding experimental curve. The details of 24 specimens collected from different research papers for the analysis are shown in Table 1.

Table 1 Details of the Specimen

S. No.	Specimen Label	Width of Specimen	Thickness of Steel Tube	Yield Strength of Steel	Compressive Strength of	Confinement Factor	P _{model} /
110.	Label	(B) (mm)	(t) (mm)	(f _{sy}) (MPa)	Concrete	(ξ)	P _{exp}
					(fck) (MPa)		
1	sczs1-1-1	120	3.84	330	18.29	2.55	1.016
2	sczs1-1-2	120	3.84	330	20.92	2.23	1.016
3	sczs1-1-3	120	3.84	330	20.92	2.23	1.063
4	sczs1-1-4	120	3.84	330	33.01	1.41	0.989
5	sczs1-1-5	120	3.84	330	35.23	1.33	1.005
6	sczs1-2-1	140	3.84	330	10.65	3.52	1.001
7	sczs1-2-2	140	3.84	330	11.21	3.34	1.037
8	sczs1-2-3	140	3.84	330	36.60	1.08	0.992
9	sczs1-2-4	140	3.84	330	36.60	1.08	0.988
10	sczs2-1-1	120	5.86	321	20.07	3.65	1.001
11	sczs2-1-2	120	5.86	321	20.07	3.65	1.047
12	sczs2-1-4	120	5.86	321	35.23	2.08	0.998
13	sczs2-1-5	120	5.86	321	35.23	2.08	1.006
14	sczs2-2-1	140	5.86	321	10.87	5.64	1.001
15	sczs2-2-2	140	5.86	321	12.22	5.02	0.995

https://doi.org/10.38124/ijisrt/25nov1123

16	sczs2-2-4	140	5.86	321	36.60	1.68	1.003
17	sczs2-3-1	200	5.86	321	11.76	3.51	0.992
18	sczs2-3-2	200	5.86	321	11.76	3.51	1.013
19	UNC25a	250	2.5	342	44.89	0.31	0.978
20	UNC25b	250	2.5	342	44.89	0.31	0.962
21	UNC19a	190	2.5	342	44.89	0.35	0.986
22	UNC19b	190	2.5	342	44.89	0.35	1.003
23	UNC19c	190	2.5	270	39.061	0.37	0.975
24	UCFT13	129.1	2.5	234.3	45.89	0.42	0.977

This procedure was repeated for all 24 specimens, generating a set of 24 data points for each parameter. In every case, the multiplied factor acts as the *dependent variable*, while the parameter on which it depends serves as the *independent variable*. Thus, for each of the three controlling parameters, a separate dataset was prepared to study their dependency relationships.

The three parameters selected for regression-based calibration are:

 η which is dependent on ε_o

 β which is dependent on confinement factor (ξ)

 σ_0 which is dependent on confinement factor (ξ)

Using the prepared datasets of independent and dependent variables, both linear and nonlinear regression analyses were performed. Among the several trial equations tested, the final equation was selected based on the criterion of achieving the minimum Residual Sum of Squares (RSS).

➤ Residual Sum of Squares (RSS)

In statistics, the *Residual Sum of Squares (RSS)* also known as the *Sum of Squared Errors (SSE)* represents the deviation of predicted values from the actual observed data. It quantifies the amount of error remaining between the

estimated regression function and the experimental dataset. A smaller RSS value indicates a better fit, meaning the model more accurately represents the experimental behavior.

➤ Regression Analysis for Peak Concavity Correction

The parameter that governs the shrinkage, expansion, or concavity of the peak region of the load–strain curve is denoted as η . This parameter is dependent on \mathcal{E}_o , and is therefore multiplied by an appropriate correction factor to ensure proper alignment with the experimental curve. For all 24 specimens, a dataset was compiled where the correction factor is treated as the dependent variable and its controlling parameter as the independent variable.

Table 2 presents the various trial equations tested along with their corresponding RSS values. In these trial formulations, $x = \xi$ (the confinement factor). The equation yielding the least RSS is considered the most suitable regression function and provides the best representation of the data trend.

> Regression Analysis for Post-Peak Residual Slope Correction

This parameter governs the post-peak residual slope of the load–axial strain curve and is dependent on the confinement factor (ξ) . To accurately replicate the experimental behaviour, this parameter is multiplied by an appropriate correction factor.

Table 2 Function Generated for Peak Concavity Correction with Corresponding RSS Values

S. No.	Functions	Residual sum of squares
1	f = 1.8269+(-292.6788)*x	1.4318
2	f = 4.3163+(1798.6509)*x+(223736.1138) *x ²	1.4090
3	$f = (-80.8602) + 75303.0979 * x + (-22816659.8978) * x^2 + 2274349818.5429 * x^3$	1.1099
4	f = (-0.1392) + (0.0032/x)	1.4241
5	$f = 0.6808 + 0.3492/(1 + e^{-((x-0.0033)/(-5.5702))})$	1.1887
6	$f = 1.3259 *x^{0.0170}/(3.6008^{0.0170} + x^{0.0170})$	1.7979
7	$f = 0.6802 * e^{(16997.0036/(x+93720.12))}$	1.7939
8	$f = 1.0373 + (-0.4865) * e^{(-0.5*)((x-0.0038))/(0.0002))}$	1.1702
9	f = 7.7594*(1-3.0977*)	2.5464
10	$f = 1.9248 + (-319.5533)*(e^{(1.337*x)} - 1)/1.337$	1.3924
11	$f = 1-1/(x^{-0.2960})$	1.7543
12	$f = (0.9309 + (-531.82) * x + 75545.63 * x^2) / (1 + (-573.13) * x + 81636.9139 * x^2)$	1.5754

13	$f = (0.4346 + (-241.6213) * x + 33756.0880 * x^2) / (1 + (-751.0106) * x + 184988.0187 * x^2 + (-14782159.70) * x^3)$	1.0460
14	$f = 0.9242 + (-1236.69)/(1 + ((x-0.0038)/4.3335)^2)$	0.9046
15	$f = 0.9134 + (-0.0048) * e^{(-0.5*(\ln(x/0.0038)/0.0044)^2)/x}$	0.8445

Using this approach, data for all 24 specimens was compiled, where the correction factor serves as the *dependent variable* and the corresponding influencing parameter acts as the *independent variable*. Table 3 presents the series of trial equations evaluated through regression analysis along with

their corresponding Residual Sum of Squares (RSS) values. In these trial equations, the value of $x = \xi$. The equation that yields the minimum RSS is considered the optimal regression function, as it provides the best statistical fit to the dataset.

Table 3 Function Generated for Post Peak Residual Slope Correction with Corresponding RSS Values

S. no.	Functions	Residual sum of squares
1	f = 3.5678+(-0.7125)*x	3.0697
2	f = x/((-0.1022) + 0.6346*x)	2.9665
3	f = 4.6482+(-2.3680)*x+0.3292*x ²	1.5977
4	f = -13179.11 + 13179.70 * x/(-8.353 + x)	1.3023
5	$f = 8.3287 * x^{-1.0046} / (0.3150^{-1.0046} + x^{-1.0046})$	1.1917
6	$f = (8.0602 + (-24.7023) * x + 6.4527 * x^2) / (1 + 0.1073 * x + (-8.9830) * x^2 + 2.5477 * x^3)$	1.1068
7	$f = (-1154.61) + 1155.4669 * (1 - e^{(-1.4708*x))^{(-0.0029)}})$	1.0887
8	$f = (7.8782 + (-26.8144) * x + 14.4161 * x^2 + (-1.8766) * x^3) / (1 + (0.3940) * x + (-8.4467) * x^2 + 5.2150 * x^3 + (-0.7034) * x^4)$	1.0752
9	$f = 5.5822 + (-4.9285) \cdot x + 1.5299 \cdot x^2 + (-0.1435) \cdot x^3$	1.0534
10	$f = 0.8741 + 6.4369 * e^{(-2.0750 * x)}$	0.9954
11	$f = 7.3110 + (-6.4369)*(1 - e^{(-2.0750*x)})$	0.9912
12	$f = 0.5007 + 6.5265 * e^{(-1.8079*x)} + 0.1039*x$	0.9821
13	$f = 1.4284 + (-2.1112/x) + (2.0896/x^2) + (-0.3466/x^3)$	0.4987
14	$f = (1.2148 + (-6.3270) * x + 14.4526 * x^2 + (-10.1339) * x^3 + 2.6942 * x^4 + (-0.2392) * x^5) / (1 + (-6.8595) * x + 15.5610 * x^2 + (-10.7813) * x^3 + 2.8463 * x^4 + (-0.2517) * x^5)$	0.4611
15	$f = (3786246 + (-21848288) * x + 29051094 * x^2 + (-37689075) * x^3 + 10341450 * x^4) / (1 + (-262237) * x + 6814966 * x^2 + (-30519675) * x^3 + 9739623 * x^4)$	0.3940

> Regression Analysis for Peak Correction

The parameter σ_o governs the peak load of the load-axial strain curve and is influenced by the confinement factor (ξ). To align the predicted curve with the experimental response, this parameter is multiplied by an appropriate correction factor. Accordingly, data for all 24 specimens was compiled, wherein the correction factor serves as the *dependent variable*, while the confinement factor acts as the *independent variable*.

Table 4 presents the various trial equations considered during the regression analysis, along with their corresponding Residual Sum of Squares (RSS). In all trial equations, the parameter $x = \xi$. The equation that produces the lowest RSS value is identified as the most suitable regression model, as it offers the best statistical fit to the dataset.

Table 4 Function Generated for Peak Correction with Corresponding RSS Values

S. no.	Functions	Residual sum of squares
1	$f = (1553.3511/x) *e^{(-0.5*(\ln(x/2541023.71)/3.8493)^2)}$	0.1570
2	$f = 1-1/(1+0.0027*x)^{31361665.37}$	0.1539
3	$f = 0.974 * x^{1.00042} / (2.292^{1.00042} + x^{1.00042})$	0.1318
4	$f = 0.6880 + 0.28*(1-e^{(-1368.68*x)})^{1651.92}$	0.1314
5	f = 0.9750 + (-0.0025) *x	0.1310
6	$f = 0.9604 + 0.0504 * 0.1476^x$	0.1277
7	$f = 0.9581 + (-0.0109) \cdot \ln(x) + 0.0127 \cdot (\ln(x))^2$	0.1270
8	$f = 0.9944 + (-0.0306) \times x + 0.0056 \times x^2$	0.1263

https://doi.org/10.38124/ijisrt/25nov1123

9	$f = 0.97 + (-0.048) \cdot \ln(x) + b \cdot (\ln(x)^2 + c \cdot (\ln(x))^3$	0.1222
10	$f = 1.0214 + (-0.1008) \times x + 0.0385 \times x^2 + (-0.0039) \times x^3$	0.1216
11	$f = 0.9940 + (-0.1144/x) + (0.0772/x^2) + (-0.0126/x^3)$	0.1185
12	$f = 0.9738* (x-3.3400)^{0.0098}$	0.1013
13	$f = 0.9604 + 0.2806 * exp^{(5*((x-4.3070)/0.1014)^2)}$	0.0763
14	f = (-4.0307 + 0.9684 * x)/(-4.1793 + x)	0.0739
15	$f = (0.9736 + (-1.8562) \times x + 0.8162 \times x^2 + (-0.1020) \times x^3) / (1 + (-1.9228) \times x + 0.8496 \times x^2 + (-0.1065) \times x^3)$	0.0613

The stress in concrete for any value of input strain may be obtained using the following equations:

$$\sigma = \sigma_o \cdot \left[A \cdot \left(\frac{\varepsilon}{\varepsilon_O} \right) - B \cdot \left(\frac{\varepsilon}{\varepsilon_O} \right)^2 \right]$$
 for $\varepsilon \le \varepsilon_o$ (1)

Where σ_o is maximum stress in filled concrete, ϵ_o is corresponding strain in concrete, ϵ_o is input value of strain for which stress to be calculated. A = 2.0 - k, B = 1.0 - k, k = 0.1 · $\xi^{0.745}$

The confinement factor (
$$\xi$$
) is defined as $\xi = \frac{A_s f_{sy}}{A_c f_{ck}}$ (2)

 A_s is the cross-sectional area of the steel tube, A_c is the cross-sectional area of the concrete, f_{sy} is the yield stress of the steel tube, and f_{ck} is the compressive strength of concrete. The value of f_{ck} is determined as 67% of the compressive strength of cubic concrete blocks.

$$\sigma = \sigma_o \cdot \left(\frac{\varepsilon}{\varepsilon_o}\right) \cdot \left[\frac{1}{\beta \cdot \left(\frac{\varepsilon}{\varepsilon_o} - 1\right)^{\eta} + \frac{\varepsilon}{\varepsilon_o}}\right]$$
 for $\varepsilon \le \varepsilon_o$ (3)

$$\sigma_o = f_{ck} \cdot \left[1.194 + 0.25 \cdot \left(\frac{13}{f_{ck}} \right)^{0.45} \cdot \left(-0.07845 \cdot \xi^2 + 0.5789 \cdot \xi \right) \right] \left(\frac{a + b.\xi + c.\xi^2 + d.\xi^3}{1 + e.\xi + f.\xi^2 + g.\xi^3} \right) \tag{4}$$

Where, a = 0.9619, b = -1.2322, c = 0.4523, d = -0.0507, e = -1.2809, f = 0.4705 and g = -0.0528 $\varepsilon_o = \varepsilon_{cc} + 0.95$

$$\left[1400 + 800 \cdot \left(\frac{f_{ck} - 20}{20}\right)\right] \cdot \xi^{0.2} \tag{5}$$

$$\varepsilon_{cc} = 1300 + 14.93 \cdot f_{ck} \tag{6}$$

$$\eta = 1.60 + 1.5 \left(\frac{\varepsilon_o}{\varepsilon} \right) \cdot \left[y_o + \left(\frac{a}{\varepsilon_o} \right) \right] \exp \left[-0.5 \left(\frac{\ln \left(\frac{\varepsilon_o}{x_o} \right)}{b} \right)^2 \right]. \tag{7}$$

Where, a = -0.0048, b = 0.0044, $x_0 = 0.0038$, $y_0 = 0.9134$

$$\beta = \left(\frac{0.75 \cdot f_{ck}^{0.1}}{\sqrt{1+\xi}}\right) \cdot \left[\frac{a+b \cdot \xi + c \cdot \xi^2 + d\xi^3 + e \cdot \xi^4}{1 + f \cdot \xi + g \cdot \xi^2 + h \cdot \xi^3 + i \cdot \xi^4}\right]$$
 for $\xi \le 3.0$

$$\beta = \left(\frac{0.75 \cdot f_{ck}^{0.1}}{\sqrt{1 + \xi} \cdot (\xi - 2)^2}\right) \cdot \left[\frac{a + b \cdot \xi + c \cdot \xi^2 + d\xi^3 + e \cdot \xi^4}{1 + f \cdot \xi + g \cdot \xi^2 + h \cdot \xi^3 + i \cdot \xi^4}\right]$$
 for $\xi \le 3.0$

a = 3786000, b = -21850000, c = 29050000, d = -37690000, e = 10340000,

f = -262200, g = 6815000, h = -30520000, i = 9740000

The units for stress and strain are in M Pa and μ m respectively.

ISSN No:-2456-2165

III. RESULTS AND DISCUSSION

The resulting load-axial strain curves obtained from the proposed model showed strong agreement with the experimental results, enabling the development of simplified

expressions for sectional capacity and load–strain behaviour. For validation purposes, specimen series *SCZS*, *UNC*, and *UCFT* were considered, which were collected from the works of Han et al. [12] and Tao et al. [13–14], respectively.

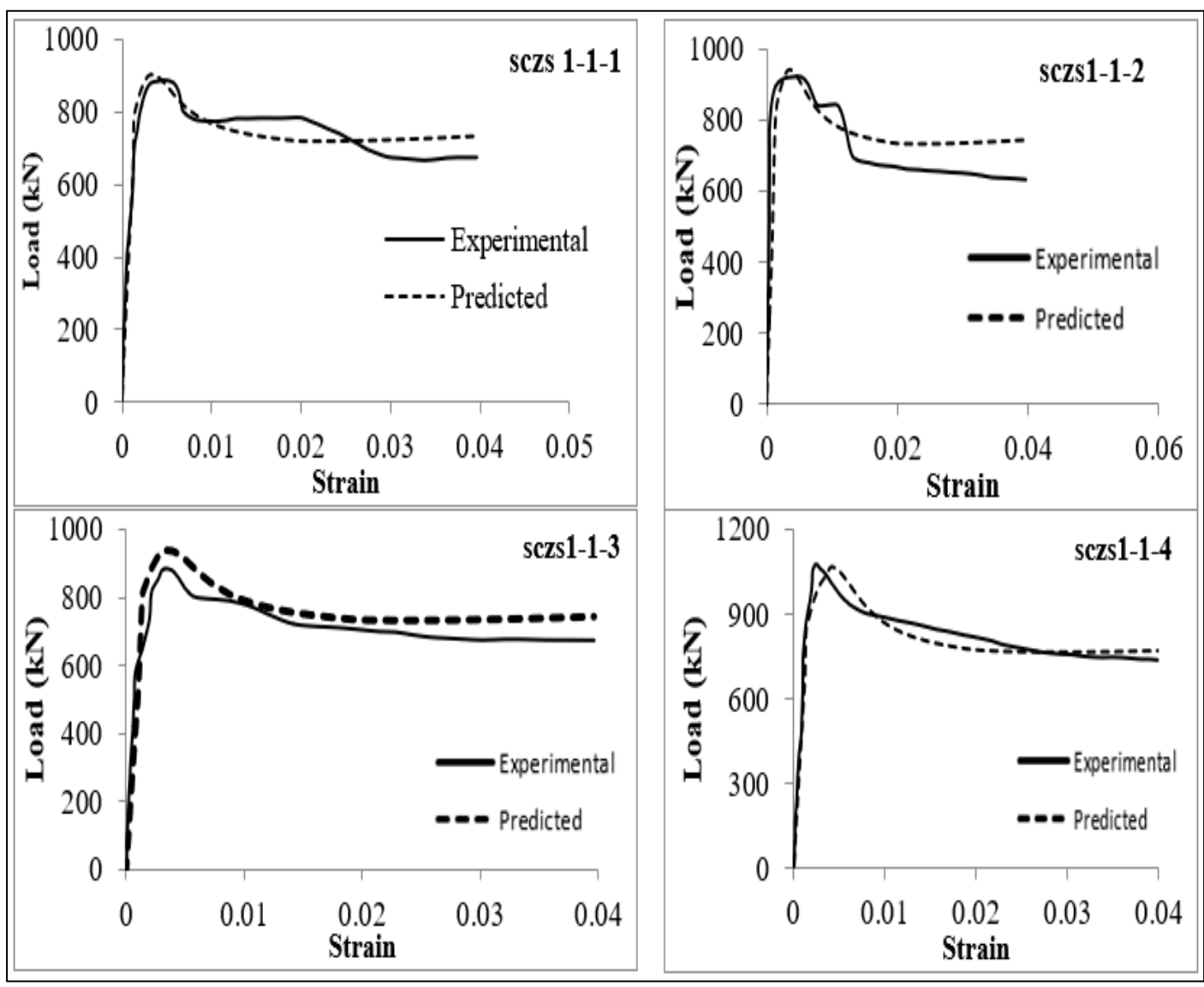


Fig 1 to 4 Validation of Results Obtained by Numerical Model with Experimental Results.

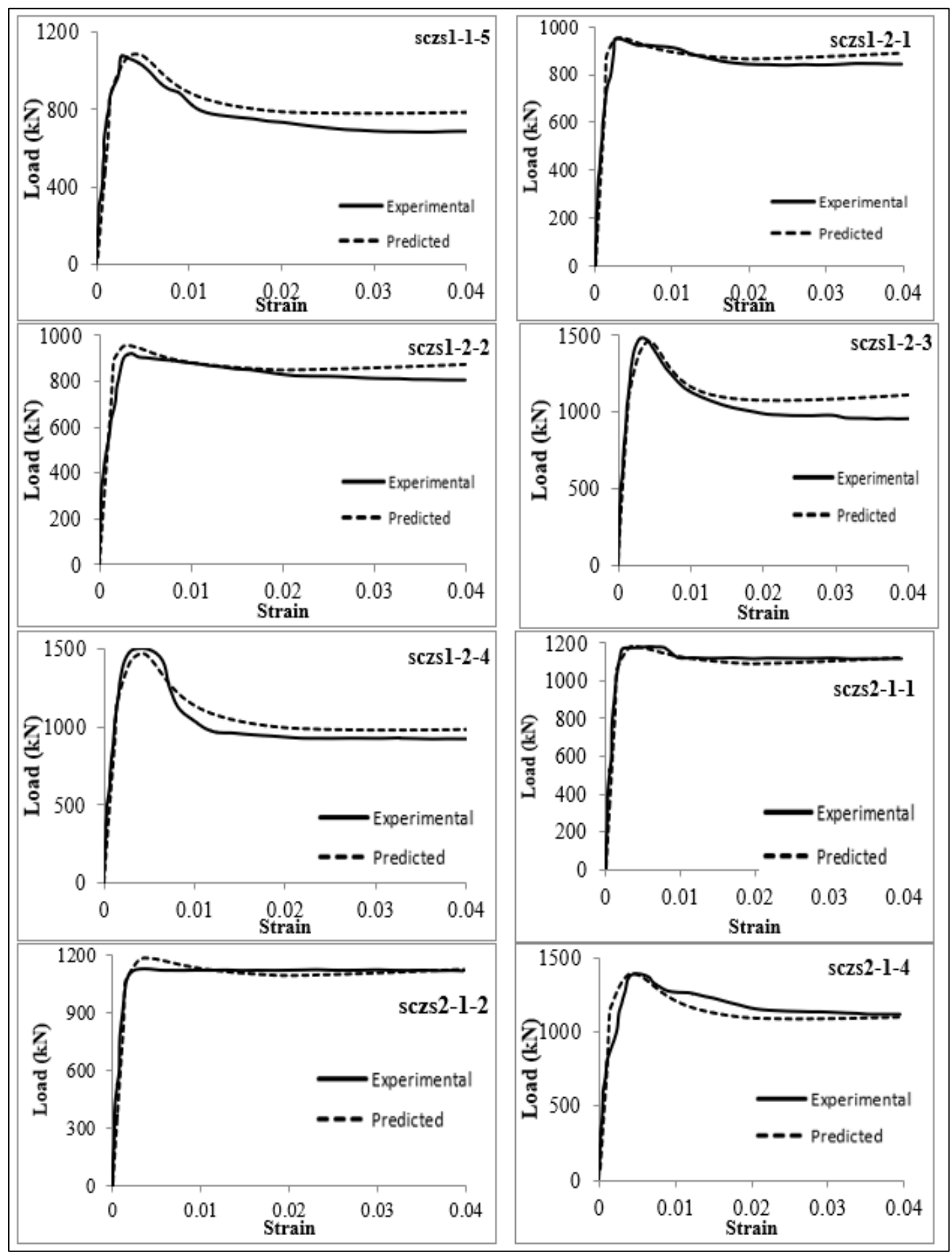


Fig 5 to 12 Validation of Results Obtained by Numerical Model with Experimental Results.

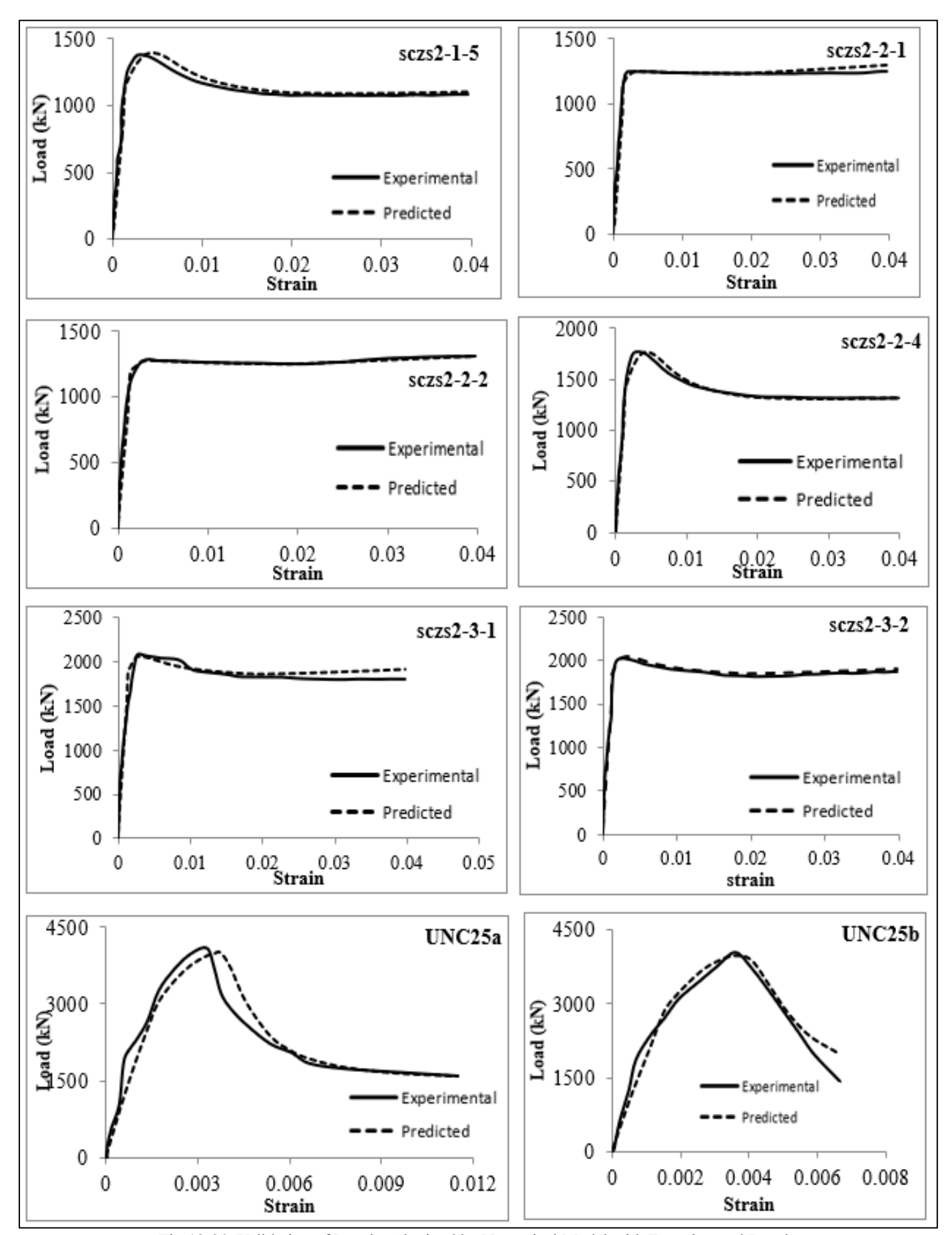


Fig 13-20 Validation of Results Obtained by Numerical Model with Experimental Results.

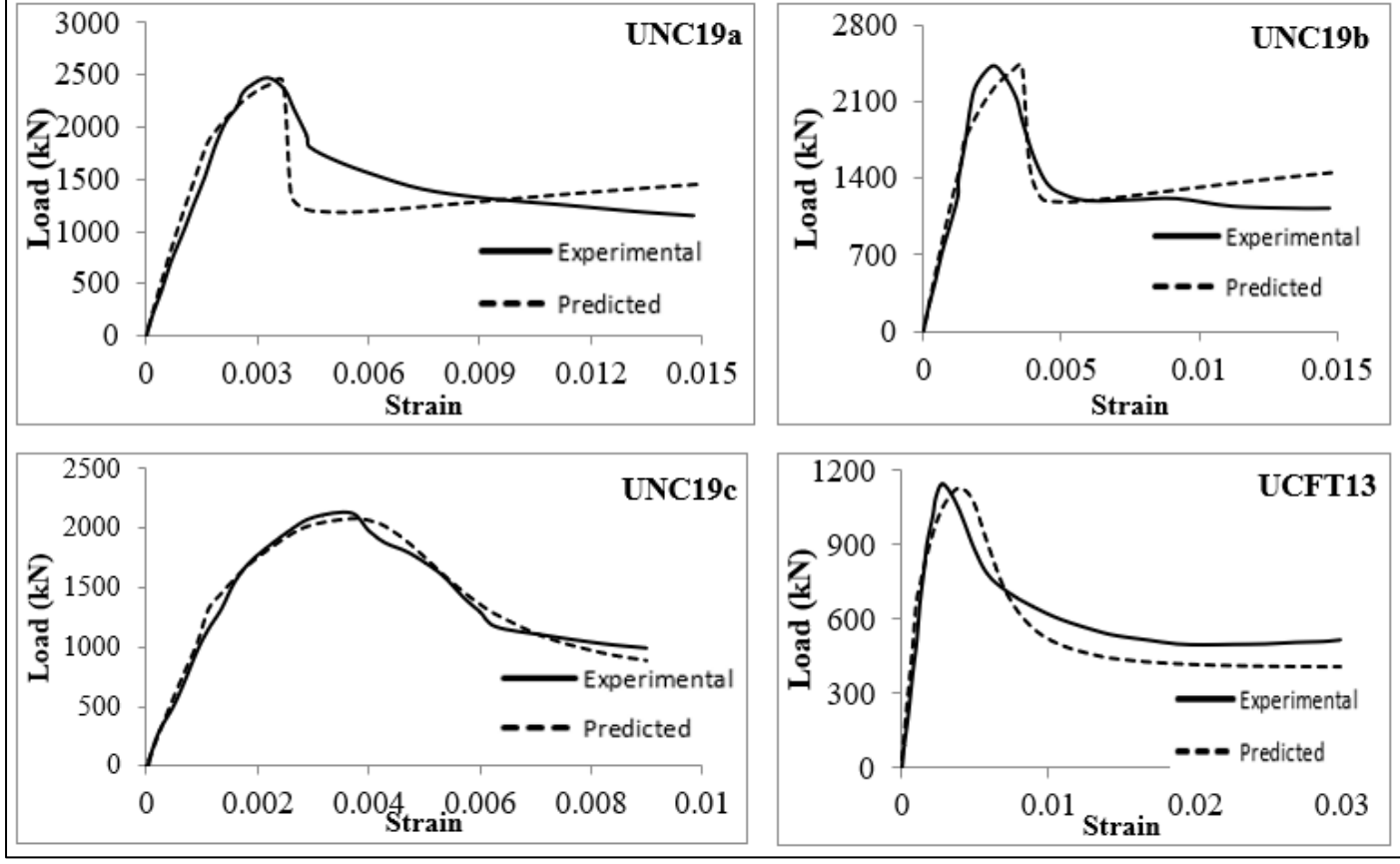


Fig 21-24 Validation of Results Obtained by Numerical Model with Experimental Results.

Comparative evaluation against 24 test results—spanning confinement factor, concrete strength and steel yield stress demonstrated excellent agreement, underscoring the reliability of the theoretical model for assessing the structural performance of square concrete-filled steel tubes in axial compression.

IV. CONCLUSIONS

- On comparing the load—axial strain curves obtained from the proposed equation with the experimental results, it can be concluded that both show good agreement, with a mean value of 1.0018, a standard deviation of 0.0227, and a coefficient of variation of 0.0226.
- It is observed that an increase in the strength of the concrete infill results in a rapid increase in the slope of the descending portion of the curve.
- Specimens with higher concrete strength exhibit strain softening after reaching the peak load.
- For most specimens, the post-peak portion of the curve becomes nearly constant due to the use of normal-strength concrete.
- Some specimens with relatively lower concrete strength exhibit strain hardening after the peak load is attained.
- All specimens were modeled using the regression-based approach, and a difference of approximately 5–10% or less was typically observed between the experimental and predicted results. These differences can be attributed to possible geometric or material imperfections.

REFERENCES

- [1]. Mander, J.B., Priestley, M.J.N. and Park, R. (1988), "Theoretical stress-strain model for confined concrete", Journal of Structural Engineering, ASCE, 114(8), 1804-1826.
- [2]. Schneider, S.P. (1998), "Axially loaded concrete-filled steel tubes", Journal of Structural Engineering, ASCE, 124(10), 1125-1138.
- [3]. Ge, H. B. and Usami, T. (1994), "Strength analysis of concrete-filled thin-walled steel box columns", Journal of Constructional Steel Research, 30, 607-612.
- [4]. Han, L.H. (1998), "Fire resistance of concrete filled steel tubular columns", Advances in Structural Engineering an International Journal, 2(1), 35-39.
- [5]. Varma AH, Ricles JM, Sause R, Lu LW. Experimental behavior of high strength square concrete-filled steel tube beam-columns. J Struct Eng 2002;128(3):309– 18.
- [6]. Yu Q, Tao Z, Wu yx.. Experimental behaviour of high performance concrete-filled steel tubular columns. Thin-Walled Struct. 2008; 46:362–70.
- [7]. Ding FX, Lu DR, Bai Y, Zhou QS, Ni M, Yu ZW, et al. Comparative study of square spiral-confined concrete-filled steel tubular stub columns under axial loading. Thin-Walled Struct. 2016; 98:443–53.
- [8]. Teng JG, Wang JJ, Lin G, Zhang J, Feng P. Compressive behavior of concrete-filled steel tubular columns with internal high-strength steel spiral confinement. Adv Struct Eng 2021;24(8):1687–708.

https://doi.org/10.38124/ijisrt/25nov1123

- [9]. Chen ZP, Jing CG, Ning P. Axial compressive behavior and parametric analysis of spiral reinforcement concrete filled square steel tubular columns. China Civ Eng J 2018;51(1):13–22.
- [10]. Tan QH, Chen ZP, Jing CG. Experimental investigation on mechanical performance and load-carrying capacity calculation of spiral-reinforced concrete-filled square steel tubular columns under eccentric compression. J Build Struct 2020;41(4): 102–9.
- [11]. Han LH, Zhao XL, Tao Z. Tests and mechanics model for concrete-filled SHS stub columns, columns and beam-columns. Steel and Composite Structures, Vol. 1, No. 1 (2001) 51-74
- [12]. Han L. H., Zhao X. L. & Tao Z. (2001). Tests and mechanics model for concrete-filled SHS stub columns, columns and beam-columns. *Steel and Composite Structures, Vol. 1, No. 1, 51-74.*
- [13]. Tao Z., Han, L. H., & Wang, Z. B. (2005). Experimental behaviour of stiffened concrete-filled thin -walled hollow steel structural (HSS) stub columns. *Journal of Constructional Steel Research*, 61(7), 962-983.
- [14]. Tao, Z., Han, L. H., & Wang, D. Y. (2008). Strength and ductility of stiffened thin-walled hollow steel structural stub columns filled with concrete. *Thinwalled structures*, 46(10), 1113-1128.